

# Naval Research Laboratory

Washington, DC 20375-5320



NRL/MR/6754-99-8368

## X-Band Microwave Properties of a Rectangular Plasma Sheet

D.P. MURPHY

R.F. FERNSLER

R.A. MEGER

*Charged Particle Physics Branch  
Plasma Physics Division*

R.E. PECHACEK

*SFA, Inc.*

*Landover, Maryland*

May 28, 1999

19990610055

Approved for public release; distribution is unlimited.

# REPORT DOCUMENTATION PAGE

Form Approved  
OMB No. 0704-0188

Public reporting burden for this collection of information is estimated to average 1 hour per response, including the time for reviewing instructions, searching existing data sources, gathering and maintaining the data needed, and completing and reviewing the collection of information. Send comments regarding this burden estimate or any other aspect of this collection of information, including suggestions for reducing this burden, to Washington Headquarters Services, Directorate for Information Operations and Reports, 1215 Jefferson Davis Highway, Suite 1204, Arlington, VA 22202-4302, and to the Office of Management and Budget, Paperwork Reduction Project (0704-0188), Washington, DC 20503.

1. AGENCY USE ONLY (Leave Blank)	2. REPORT DATE	3. REPORT TYPE AND DATES COVERED	
	May 28, 1999	Interim	
4. TITLE AND SUBTITLE  X-Band Microwave Properties of a Rectangular Plasma Sheet			5. FUNDING NUMBERS  JO #67-7641-A9
6. AUTHOR(S)  D.P. Murphy, R.F. Fernsler, R.E. Pechacek,* and R.A. Meger			
7. PERFORMING ORGANIZATION NAME(S) AND ADDRESS(ES)  Naval Research Laboratory Washington, DC 20375-5320			8. PERFORMING ORGANIZATION REPORT NUMBER  NRL/MR/6754--99-8368
9. SPONSORING/MONITORING AGENCY NAME(S) AND ADDRESS(ES)  Office of Naval Research 800 North Quincy Street Arlington, VA 22217-5660			10. SPONSORING/MONITORING AGENCY REPORT NUMBER
11. SUPPLEMENTARY NOTES  *SFA, Inc., Landover, MD 20785			
12a. DISTRIBUTION/AVAILABILITY STATEMENT  Approved for public release; distribution is unlimited.			12b. DISTRIBUTION CODE
13. ABSTRACT (Maximum 200 words)  Detailed scans of x-band microwave transmission, reflection and noise emission of various Agile Mirror plasma sheets as a function of frequency have been performed. The reflected microwave signal from the plasma sheet is compared to that reflected from an aluminum plate with the same dimensions as the plasma. Estimates of the electron density are made by measuring the transmission through plasma sheets that are then compared to x-band wavelengths. The noise spectrum is mapped, and mechanisms that might produce this noise are discussed.			
14. SUBJECT TERMS  Plasma X-band Microwave			15. NUMBER OF PAGES 24
			16. PRICE CODE
17. SECURITY CLASSIFICATION OF REPORT  UNCLASSIFIED	18. SECURITY CLASSIFICATION OF THIS PAGE  UNCLASSIFIED	19. SECURITY CLASSIFICATION OF ABSTRACT  UNCLASSIFIED	20. LIMITATION OF ABSTRACT  UL

## CONTENTS

ABSTRACT . . . . .	1
INTRODUCTION . . . . .	1
MICROWAVE REFLECTION FROM A PLASMA . . . . .	1
PLASMA MODES . . . . .	2
MICROWAVE APPARATUS . . . . .	3
REFLECTION MEASUREMENTS FROM A METAL PLATE . . . . .	4
TRANSMISSION AND REFLECTION MEASUREMENTS OF PLASMA SHEETS . . . . .	5
MICROWAVE NOISE MEASUREMENTS OF PLASMA SHEETS . . . . .	6
SUMMARY AND CONCLUSIONS . . . . .	8
APPENDIX—Agile Mirror Electron Density as Derived from Microwave Transmission Measurements . . . . .	9

# X-Band Microwave Properties of a Rectangular Plasma Sheet\*

D. P. Murphy, R. F. Fernsler, R. E. Pechacek<sup>a</sup> and R. A. Meger

*Plasma Physics Division, Code 6750*

*Naval Research Laboratory, Washington, DC 20375-5346*

## ABSTRACT

Detailed scans of x-band microwave transmission, reflection and noise emission of various Agile Mirror plasma sheets as a function of frequency have been performed. The reflected microwave signal from the plasma sheet is compared to that reflected from an aluminum plate with the same dimensions as the plasma. Estimates of the electron density are made by measuring the transmission ratio through plasma sheets that are thin compared to x-band wavelengths. The noise spectrum is mapped and mechanisms that might produce this noise are discussed.

## INTRODUCTION

Sheet plasmas were produced in the Agile Mirror chamber using a 60 cm long by 1.9 cm diameter stainless steel tubular cathode with a 1 cm wide slot cut lengthwise. The anode-cathode (AK) gap is 60 cm also. The fill gas in the chamber was oxygen at pressures of 20-100 mTorr. A Crossatron<sup>1</sup>-switched capacitor bank was used to deliver a high voltage pulse that is set typically at 300  $\mu$ s length<sup>2</sup>. The capacitor bank was charged to 2000-5000 volts. There was 80 ohms series resistance in the output circuit to limit the maximum discharge current. A magnetic field up to 310 gauss with  $\pm 5\%$  uniformity was applied over the plasma volume using a pair of 60 cm radius Helmholtz coils. A hollow cathode was used in order to increase the beam current and thus the plasma produced as the beam ionizes the background gas.<sup>3</sup> The magnetic field confines the beam electrons produced by the hollow cathode. For high magnetic fields, the beam electrons are emitted only along the edges of the cathode slot, so the plasma consists of two thin sheets a few millimeters thick. At low magnetic fields, the beam electrons are scattered by the background gas so the plasma is spread out to a thickness of several centimeters or more at the anode. Normally the system is operated at moderate magnetic field values of 200-280 gauss, which produces a uniform plasma nominally 1 cm thick from top to bottom.

## MICROWAVE REFLECTION FROM A PLASMA

Electromagnetic waves are reflected from a thick plasma when the frequency is less than or equal to the plasma frequency (see figure 1). The plasma frequency  $\omega_{pe} = (4\pi e^2 n_e / m_e)^{1/2}$  radians/sec is determined by the electron density,  $n_e$ , where  $e$  is the electronic charge and  $m_e$  is the mass of the electron. This determines a critical

\* Work supported by the Office of Naval Research

<sup>a</sup> SFA, Inc., Landover, MD 20785

Manuscript submitted April 8, 1999.

electron density  $n_e \cong 1.23 \times 10^{12} (f_{\text{GHz}} / 10)^2 \text{ cm}^{-3}$ , where  $f_{\text{GHz}}$  is the incident frequency in gigahertz. The Agile Mirror plasma sheet is produced by propagating a beam of kilovolt electrons through a low pressure background gas. Ionization by high energy electrons is an efficient process, allowing a low current density beam to produce a high plasma density. A 3 kV electron can propagate through  $\sim 1$  meter of gas at pressures below 100 mTorr before it loses most of its energy to collisions. The high energy electrons are generated in the cathode sheath region. Electrons produced by collisions outside the sheath region are not accelerated to high energy and are therefore not able to efficiently ionize the background gas in the AK gap. Even at its highest electron density, however, the gas is only weakly ionized ( $n_e/n_0 < 10^{-3}$ ,  $n_0$  = neutral gas density).

In the low pressure regime used in these experiments, the absorption of microwave energy by the plasma is weak. The ratio of the electron-neutral collision frequency to the wave or plasma frequencies is ( $\% \ll 1$ ), so collisional damping is small provided the underdense wings of the plasma are less than an electromagnetic skin depth,  $(c/\omega_{pe})$  thick. X-band microwaves are of  $\sim 3$  cm wavelength, so the plasma sheets are usually thin compared to the incident radiation wavelength. The predominate plasma decay mechanism is two-body recombination between electrons and ions for Agile Mirror operation in oxygen. Calculations indicate that a  $10^{12} \text{ cm}^{-3}$  electron density should decay with a half time of  $\sim 10 \mu\text{sec}$ .

### PLASMA MODES

The Agile Mirror has been operated with bank voltages of 2-5 kV and oxygen pressures of 20-100 mTorr. A white, negative-glow (NG) plasma fills the AK gap. Typically, four discharge modes are observed, depending on the fill gas pressure and the magnetic field strength. Each mode has its distinct visual and current characteristics. The modes are designated the Abnormal Glow (AG), the Unmagnetized Hollow Cathode (UHC), the Positive-Column (PC) and the Enhanced Glow (EG) modes. Figure 2 shows a map of the plasma modes at a bank voltage of 2600 Volts as a function of the background pressure, magnetic field and discharge current. The maps are similar at other charge voltages. Below  $\sim 50$  mTorr, the modes change abruptly with magnetic field variations as small as 1%.

In the Abnormal Glow mode it is theorized that the hollow-cathode effect does not take place, and thus that there are few high energy electrons to ionize the gas in the AK gap. The plasma electron density is therefore low and the plasma sheet is transparent to x-band microwaves. The plasma sheet has a high measured impedance ( $V/I \sim 1.5-3 \text{ k}\Omega$ ). The plasma current is about 2 amps even though most of the bank voltage is dropped across the AK gap.

In the UHC mode it is theorized that electrons emitted from the surface inside the hollow cathode region have a large gyroradius. They thus reflex back and forth several times through the sheaths on both sides of the slotted region before escaping to ionize the gas in the AK gap. However, the beam electrons are not well confined in the low magnetic field. The peak electron density in the broad discharge is not

high enough to make a good microwave reflector even though the discharge current is relatively high ( $I \sim 10$  A) and the impedance low ( $V/I \sim 100 \Omega$ ).

At high magnetic field, a mode develops in which a positive-column region, 10-30 cm high, forms above the anode. The plasma sheath in the hollow cathode region collapses and the gap potential falls to a few hundred volts. The discharge current is limited primarily by the external impedance of the Crossatron switch system. The impedance of the plasma sheet is only  $30-40 \Omega$ . The low energy beam electrons that emerge from the slot are scattered before they can fully cross the anode-cathode gap. This results in a non-uniform plasma distribution with a strong electron density gradient in the vertical direction. Thin, bright plasma sheets originate on the edges of the slot, but they fade rapidly after a few centimeters. With oxygen, the NG region is white (from  $O_2^+$  emission) and the PC region is white, but much dimmer (from molecular  $O_2$  emission). If nitrogen is introduced into the chamber, the NG region is purple (from  $N_2^+$  emission) and the PC region is orange (from molecular  $N_2$  emission).

Plasma production was found to be most efficient in the Enhanced Glow mode with a magnetic field of 200-280 gauss. The sheath thickness and the electron gyroradius inside the hollow cathode region seem well paired for the production of kilovolt energy electrons. The discharge current is only about a factor of two larger than that in the Abnormal Glow mode but the impedance is still adequately large, ( $V/I \sim 200-300 \Omega$ ) while the plasma electron density is many times higher. Electron densities as high as  $3 \times 10^{12} \text{ cm}^{-3}$  have been measured. At higher pressures ( $>60$  mTorr), as the magnetic field is decreased there is a smooth transition from the EG mode to the UHC mode without passing through the Abnormal Glow mode. The discharge current rises but the plasma density falls with decreasing magnetic field at these pressures.

### MICROWAVE APPARATUS

The X-band source for this experiment is an HP 8690B that is AM modulated at 50 kHz by an HP 214A pulse generator. Pyramidal, 20db gain antennas are used to transmit and receive the signals. The AM modulated signals are measured using HP 8474B crystal detectors and recorded on a LeCroy 9314 digital oscilloscope. The experimental setup for the transmission and reflection measurements is depicted in figure 3. The spontaneous noise signals were detected by another pyramidal antenna aimed at the plasma sheet. The noise signal was mixed with a local oscillator signal from an HP 83630A microwave source to down convert to a  $\pm 40$  MHz bandwidth signal centered at the local oscillator frequency. The down converted signals were recorded using a LeCroy 9314 digital oscilloscope. The experimental setup for the noise measurement is depicted in figure 4. The pyramidal antennas were mounted more than 80 cm from the center of the chamber, which is a sufficient distance to ensure that the plasma sheet is in the far-field pattern of the antennas. However, the chamber walls, the Helmholtz magnetic

field coils and other supports that were in the field of view of the horns had to be taken into account for the reflected microwave measurements.

#### REFLECTION MEASUREMENTS FROM A METAL PLATE

Preliminary measurements of the microwave signals reflected directly back from a dense plasma sheet showed an anomalous frequency dependence. In order to determine the source of this anomalous behavior a series of tests were conducted using a flat aluminum plate in place of the plasma sheet. The aluminum plate was suspended from the cathode and was nominally identical in size to the plasma sheet. Five test runs were performed stepping through the X-Band region of 8.5 GHz to 12.0 GHz in 0.05 GHz increments. See figures 5a through 5e for the experimental setup and figures 6a and 6b for the test results.

1. Trace (Out/In)Arnd corresponds to the situation where the In and Out horns are placed 164 cm apart, directly facing each other with nothing in between them but air. The horns are standard 20 db pyramidal shaped, X-Band horns. The gain actually varies from ~18 db to ~22 db, linearly with frequency. The In signal is measured using a 10 db directional coupler mounted in the transmission line before the source signal reaches the In horn, so this signal is independent of the gain of the horn. The Out signal is normalized to the In signal at each frequency step. The (Out/In)Arnd trace rises smoothly with frequency due to the small increase in horn gain (directivity) with frequency.
2. Trace (Out/In)SW corresponds to the situation where the In and Out horns are placed 164 cm apart, directly facing each other with a single section of cylindrically shaped, 1.23 cm thick polycarbonate plastic placed between the two horns in the position corresponding to one wall of the chamber. The polycarbonate piece is a spare half section of chamber wall in pristine condition. The (Out/In)SW trace is smaller than the (Out/In)Arnd trace by ~10% to 30%, depending on the frequency. This indicates that the wall material is not 100% transparent at X-Band frequencies. The losses are due to both absorption and reflection.
3. Trace (Out/In)Thru corresponds to the situation where the In and Out horns are placed 164 cm apart, directly facing each other, on opposite sides of the cylindrically shaped, 80 cm diameter Agile Mirror chamber. There is no aluminum plate and no plasma within the chamber during this data run. The chamber walls are coated with evaporated metal from several years of operation of the Agile Mirror electrodes and can not be readily cleaned. The (Out/In)Thru trace is ~30% to 50% smaller than the (Out/In)Arnd trace. The variation with frequency is more pronounced.
4. Trace (Out/In)135 corresponds to the situation where the aluminum plate is suspended from the cathode. The In and Out horns are situated at  $\pm 22.5^\circ$  from normal incidence to the plate (see Fig. 5d). The angle between the original direction vector and the reflected direction vector is  $135^\circ$  (i.e., the included angle between the horns is  $45^\circ$ ). The path length between the horns is 164 cm. The mean trace value is down by more than a factor of 3 from the (Out/In)Arnd

levels, with a variation about the mean of more than 50%. The variation with frequency now has a significant, periodic component that may be due to an interference pattern developing within the region between the two horns. If we

solve the equation,  $L = \frac{n\lambda_1}{2} = \frac{(n+1)\lambda_2}{2}$ , by inserting the wavelengths

corresponding to adjacent peaks in the (Out/In)135 trace, we obtain  $L = 38 \pm 1$  cm. This agrees with the distance from the center of the plate to the inside of the Agile Mirror chamber wall. When the distance from the plate to the chamber wall was decreased by 0.5 cm the peaks in the amplitude versus frequency plot shifted position and were more closely spaced, corresponding to a 1 cm decrease in the path length.

5. Trace (Out/In)180 corresponds to measurements for which the aluminum plate is suspended from the cathode and the microwave signal is directed at the aluminum plate at normal incidence. Only one horn is used. The Out signal is derived from a second, 10 db directional coupler mounted in the transmission line used to collect signals reflected directly back into the horn from the chamber and plate. There is a strong periodic structure in the return signal and the amplitude varies by more than a factor of 100! The interference evident when the microwave signal is reflected back into the source horn makes it impossible to measure the reflection coefficient for near normal incidence.

The periodic structure observed in the microwave signals that pass in and back out of the Agile Mirror chamber complicates the measurement of the reflection coefficient of a plasma sheet as a function of frequency. It was determined in Test setup #4 that a small change in the distance between the reflector and the chamber walls affected the spacing between peaks in the reflected signal as a function of frequency. In a radar application of the Agile Mirror, slight changes in the operating conditions would shift the critical density surface within the plasma relative to the chamber walls. The acrylic material used for the vacuum shell of the Agile Mirror, while providing good diagnostic access to the plasma, is inappropriate for actual radar applications because it has a relatively high reflection coefficient in the X-Band region.

#### TRANSMISSION AND REFLECTION MEASUREMENTS OF PLASMA SHEETS

Simultaneous measurements of the transmitted and reflected signals from an Enhanced Glow plasma sheet ( $B=235$  G,  $P=50$  mTorr  $O_2$ ,  $V=3000$ ) were recorded. The sheet was 60 cm wide by 60 cm high by 1 cm thick. The signal source horn and the transmitted signal horn faced each other on opposite sides of the Agile Mirror chamber. They were each 90 cm from the chamber axis. The reflected signal horn pointed at the chamber axis, in the same plane as the source and transmitted signal horns, but was mounted  $45^\circ$  around the chamber from the source horn. Its distance from the chamber axis was also 90 cm. The cylindrical, hollow cathode was rotated  $22.5^\circ$  to the normal between the source and transmitted signal horns so that microwaves reflected from the plasma sheet would enter the reflected signal horn. This rotation of the plasma sheet increases the path length through the plasma by

about 10%. After the plasma sheet measurements were completed, the procedure was repeated with no plasma present and again with an aluminum plate suspended from the cathode. The plate duplicated the plasma sheet dimensions. Figure 7 presents the reflected signals as a function of frequency from the aluminum plate in the chamber, the plasma sheet in the chamber and the bare chamber. These signals are normalized to the source signal amplitude. The ratio of the transmitted signal with and without plasma as a function of frequency is also plotted. The transmission ratio can be used to determine the plasma frequency and the peak electron density in the sheet. Since the sheet is thin compared to the incident signal wavelength, the calculation must account for evanescent waves penetrating the sheet at frequencies below the plasma frequency (see Appendix). For these plasma conditions the calculated electron density is  $2 \times 10^{12} \text{ cm}^{-3}$  with a plasma frequency of 12.4 GHz.

#### MICROWAVE NOISE MEASUREMENTS OF PLASMA SHEETS

The spontaneous microwave emission from EG mode plasma sheets was measured within the X-band spectrum, since any extraneous microwaves from the sheet could limit the sensitivity of a radar system to detect incoming targets. The theory of microwave emission from the Agile Mirror has evolved steadily over the past several years. It was initially believed that any emission from the sheet would be *Bremsstrahlung* radiation from collisions between plasma electrons and neutral gas particles. Such emission would be broad band and come mainly from the underdense plasma wings. Its radiation temperature would be a small fraction of the electron temperature, since the plasma is a good reflector and thus a weak emitter. The signal level was expected to be only be 2-3 times background levels or less. Unfortunately, experimental measurements of the spontaneous emission from the EG mode plasma sheets disproved this postulate. The radiated power was 4-8 times the background level and there was a sharp drop-off in emission above the plasma frequency (see fig. 8). Figure 8 shows the current trace vs time from a 300  $\mu\text{s}$  long, EG mode discharge along with the noise power (in arbitrary units), measured at 10, 11 and 12 GHz. The plasma frequency is about 11 GHz under these conditions. Emission at 10 GHz and below is 4-8 times background throughout the pulse. Emission at 11 GHz is high until halfway through the pulse when the discharge current drops by about 10% and the emission then drops to background level. It is believed the drop in current follows a drop in electron density and a corresponding drop in the maximum plasma frequency ( $f_{pe} = 8.98 \times 10^3 \sqrt{n_e} \text{ Hz}$ ) to below 11 GHz. Emission at 12 GHz is indistinguishable from background level. The sharp drop in emission above  $f_{pe}$  suggests a two-stream instability between beam electrons and plasma electrons is the source. The two-stream instability converts beam energy into microwaves at the local  $f_{pe}$ , so the spontaneous radiation intensity drops to background levels above the peak  $f_{pe}$ .

If the source driving the emission is the two-stream instability, the emission spectrum should be appreciable at and below the maximum  $f_{pe}$  and that the electric field of the emitted radiation should be parallel to the external magnetic field. By design, the pyramidal, 20db microwave horns used in these experiments had always been so oriented. Figure 9 shows a plot of emission data as a function of detector frequency for a series of EG mode discharges (250 gauss, 40mT O<sub>2</sub>, V<sub>capacitor</sub>=3000 volts) and a series of AG mode discharges (150 gauss, 40mT O<sub>2</sub>, V<sub>capacitor</sub>=3000 volts). The emission signal for each discharge is reduced to a single data point by averaging the noise power over the entire 300  $\mu$ s pulse. The amplitude is proportional to the total emission at the detector frequency during the pulse and various geometric factors which are constant during this scan. The AG mode data is included in Figure 9 as a point of reference. The AG discharges are completely transparent to x-band microwaves so their local  $f_{pe}$  is much lower than the detector setting ( $f_{pe} \ll f_{det}$ ). Therefore, the noise from the AG discharges should be and is very near to the background values. The EG mode data was taken using a 0.25 GHz interval and shows features with about a 0.75 GHz spacing that are 4-6 times larger amplitude than background levels. The EG mode signals do however drop to background levels for detector settings well above the maximum  $f_{pe}=10$  GHz. This variation with frequency was not predicted by the two-stream instability hypothesis. Moreover, the emission was expected to be polarized along the direction of the external magnetic field, with little emission detected with the pyramidal horn perpendicular to the magnetic field.

Figure 10 shows data from two EG mode data runs (250 gauss, 40mT O<sub>2</sub>, V<sub>capacitor</sub>=3000 volts, 0.1 GHz intervals), one with the detector horn in the standard orientation and one with the detector horn rotated 90°. Instead of being weaker, the emission polarized perpendicular to the external magnetic field was stronger and as much as 25 times background levels. The spacing between peaks is about 0.7 GHz which is the electron gyrofrequency ( $f_{ce}$ ) in a 250 gauss magnetic field ( $\pm 5\%$ ) so the peaks probably correspond to harmonics of  $f_{ce}$ . The peak near 9.7 GHz would be about the 14<sup>th</sup> harmonic of  $f_{ce}$ . A second EG mode data series was taken at a slightly lower magnetic field (235 gauss, 40mT O<sub>2</sub>, V<sub>capacitor</sub>=3000 volts, 0.1 GHz intervals). Figure 11 shows the emission polarized perpendicular to the magnetic field for both 235 and 250 gauss. The emission peaks at 235 gauss are shifted to lower frequencies and have a reduced spacing relative to the 250 gauss data. This is consistent with a lower  $f_{ce}$  at 235 gauss.

A Helmholtz pair of coils produces the magnetic field for the Agile Mirror experiment. While this allows good external access to the plasma sheets, the magnetic field bows outward between the coils and is only  $\pm 5\%$  uniform over the plasma volume. The variation in magnetic field strength would cause the emission peaks to be broadened. Plasma emission perpendicular to the magnetic field was described in a paper by G. Landauer, et al. (Proc. 5<sup>th</sup> Int. Conf. On Ionized Phen. In Gases, Vol. I, p. 389 (1961)). In this paper, sharp peaks up to the 45<sup>th</sup> harmonic of

$f_{ce}$  were measured as the external magnetic field was varied from 0 to 2000 gauss. Analysis of this and other similar experiments was presented in papers by Canobbio and Croci (Proc. 6<sup>th</sup> Int. Conf. On Ion. Phen. In Gases, Vol. III, p. 269 (1963)) and T. H. Stix (Phys. Rev. Lett. **15**, p. 878 (1965)). They attributed the emission to *Bernstein* waves excited by super-thermal (beam) electrons. *Bernstein* waves are electrostatic, move across B, and exhibit sharp resonances at harmonics of  $f_{ce}$ . The mechanism which might divert energy from the longitudinal, two-stream instability into perpendicular *Bernstein* waves is undetermined.

### SUMMARY AND CONCLUSIONS

Although the physical characteristics of the Agile Mirror chamber complicated reflection measurements, the data indicates that below the peak plasma frequency, the plasma sheet reflected just like a metal plate of the same size. Microwave transmission measurements directly through the chamber were used to determine the peak electron density, after taking into account the plasma thinness. The calculated electron density was consistent with the observed reflection characteristics. The spontaneous microwave emission spectrum and strength were larger than expected, and the noise signal polarized perpendicular to the external magnetic field was as much as 25 times higher than background. In any potential radar application scenario in which the plasma sheet is deflected in an arbitrary direction, a component of the magnetic field will be oriented perpendicular to the polarization of the detector horn. Such high emission in the detector's frequency band from a beam-ionized plasma sheet would severely limit this type of Agile Mirror's usefulness as a beam director in radar applications.

## APPENDIX

### Agile Mirror Electron Density as Derived from Microwave Transmission Measurements

The cutoff of microwave transmission through the Agile Mirror plasma sheet has been used to estimate the peak electron density in the sheet. In general, the microwave source frequency is adjusted so that transmission at normal incidence is completely stopped by the plasma sheet and the electron density then estimated from  $f = 8.98 \times 10^3 \sqrt{n_e} \text{ Hz}$ . That is, a cutoff at 10 GHz implies a peak electron density of  $1.2 \times 10^{12} / \text{cc}$ . That method significantly underestimates the actual plasma density when the plasma is thin. The tubular cathodes used in the Agile Mirror have a slit width of  $\sim 1\text{cm}$ , which is one-third the wavelength of 10 GHz microwaves.

Evanescnt waves can penetrate the plasma sheet and be detected on the far side even if the plasma density is above cutoff.

This calculation follows the procedure developed in Corson & Lorrain's *Introduction to EM Fields and Waves*, p392-396.<sup>4</sup> There the penetration of an EM wave through a thin conducting sheet is derived. In MKS units the average value of the Poynting vector incident on the front surface is

$$S_i = \frac{1}{2} \operatorname{Re}(E_i \times H_i^*) = \frac{1}{2} \left( \frac{\epsilon_o}{\mu_o} \right)^{\frac{1}{2}} E_{oi}^2 . \quad (\text{A1})$$

Inside the sheet, just before the back surface, the average value is  $S_t$ , where

$$S_t = \frac{1}{2} \operatorname{Re}(E_t \times H_t^*) = 2^{\frac{1}{2}} \left( \frac{\omega \epsilon_o}{\sigma} \right)^{\frac{1}{2}} e^{-2\frac{1}{2}\delta} S_i . \quad (\text{A2})$$

Outside the sheet, just after the second surface, the average value is  $S_{tt}$ , where

$$S_{tt} = \frac{1}{2} \operatorname{Re}(E_{tt} \times H_{tt}^*) = \left[ 2^{\frac{1}{2}} \left( \frac{\omega \epsilon_o}{\sigma} \right)^{\frac{1}{2}} \right] \left[ e^{-2\frac{1}{2}\delta} \left[ 2^{\frac{1}{2}} \left( \frac{\omega \epsilon_o}{\sigma} \right)^{\frac{1}{2}} \right] S_i \right] = 16 \left( \frac{\omega \epsilon_o}{\sigma} \right) \left( e^{-2\frac{1}{2}\delta} \right) S_i . \quad (\text{A3})$$

Here "a" is the width of the conductor,  $\sigma$  is its conductivity and  $\delta$  is the penetration depth of the microwaves at frequency  $f = \omega / 2\pi$ . Following the derivation in *Corson and Lorrain*, the conductivity of tenuous plasma is  $\sigma \approx -j \frac{n_e e^2}{m_e \omega}$ . The penetration depth<sup>5</sup> is

$$\delta_{plasma} = \frac{c}{\sqrt{\omega_p^2 - \omega^2}} \text{ for } \omega < \omega_p . \quad (\text{A4})$$

In MKS units  $\omega_p^2 = \frac{n_e e^2}{m_e \epsilon_0}$ . Note that the term  $e^{-2x/\delta}$  in equation (A3) comes from

the integration through the plasma of the equation  $1 - \int_0^a \frac{d}{dx} [e^{-2x/\delta}] dx$ , with the

assumption that  $n_e$  is constant and therefore  $\delta$  is also constant. If  $n_e$  is not constant then the derivative  $\frac{d}{dx} [e^{-2x/\delta}]$  must be evaluated before integration:

$$\frac{d}{dx} [e^{-2x/\delta}] = [e^{-2x/\delta}] \left[ \frac{-2}{\delta} + x \frac{2}{\delta^2} \frac{\partial \delta}{\partial \omega_p} \frac{d\omega_p}{dx} \right] = \left[ \frac{-2}{\delta} \right] [e^{-2x/\delta}] \left[ 1 + \frac{2x e^2}{(\omega_p^2 - \omega^2) \epsilon_0 m_e} \frac{dn_e}{dx} \right]. \quad (A5)$$

However, the correction term in the last bracket,  $\frac{2x e^2}{(\omega_p^2 - \omega^2) \epsilon_0 m_e} \frac{dn_e}{dx} \approx \frac{2x}{N_e} \frac{dn_e}{dx}$ , is probably small if the gradient is not too sharp or the density peaked in the center.

A better estimate of the plasma electron density is obtained by using a modified equation for the penetration depth that accounts for collisions;

$$\delta_{plasma} = k^{-1}$$

$$c^2 k^2 = \frac{(\omega_p^2 - \omega^2 - v^2)}{2} + \sqrt{\left( \frac{(\omega_p^2 - \omega^2 - v^2)}{2} \right)^2 + \left( \frac{v \omega_p^2}{2 \omega^2} \right)^2} \quad (A6)$$

where,  $v$  is the electron-neutral collision frequency and  $c^2 k^2$  is real even when  $\omega > \omega_p$ . It is this form of the dispersion relation that is used to calculate the penetration depth.

Assuming the correction for non-uniform electron density is small, the plasma electron density can be estimated from the data shown in figure A1. The figure shows the transmission through the plasma at normal incidence of a chopped microwave signal and the plasma current as a function of time. The microwave source is pulsed on and off at a 50 kHz rate. It takes about 40  $\mu$ sec to fully establish the dense plasma sheet. Some of the 11GHz microwave signal bleeds through the plasma sheet throughout the entire pulse. Based on the assumption that complete reflection occurs for  $f = 8.98 \times 10^3 \sqrt{n_e}$ , one would calculate that the density is less than  $1.5 \times 10^{12} \text{ cm}^{-3}$ . If one instead evaluates the data using equations (A3) and (A6), the estimated density is considerably higher. The transmission ratio varies from about 4.9% early in the pulse to about 9.7% late in the pulse. This would imply from (A3) that the density peaks at  $\approx 3.3 \times 10^{12} \text{ cm}^{-3}$  early in the pulse and falls to  $\approx 2.9 \times 10^{12} \text{ cm}^{-3}$  just before the current pulse ends. Over that same time the plasma current drops from 12.9 Amps to 11.6 Amps. Thus, both the electron density and the plasma current experience about a 10% decay. After the external current pulse is turned off it takes about 50  $\mu$ sec for the attenuation of the microwave signal to

disappear in this shot. A 50  $\mu$ sec decay time is not inconsistent with the recombination rate for an oxygen plasma with a background pressure of 31 mTorr. The decay time depended on the plasma conditions.

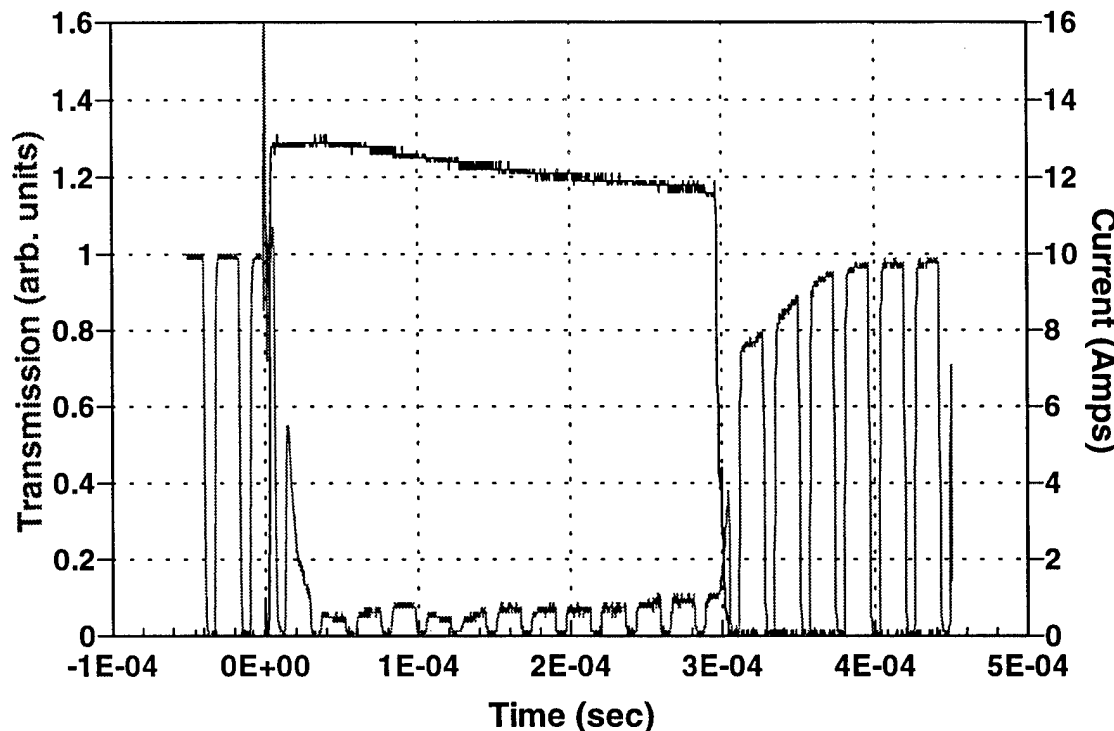


Figure A1. A plot of the plasma current and the microwave transmission for an EG mode plasma. Source frequency is 11 GHz. The background gas is oxygen at 31 mTorr (4.13 Pa). The magnetic field is 280 gauss ( $2.8 \times 10^{-2}$  T) and the capacitor bank charge voltage is 3.5 kV.

# MICROWAVE INTERACTION WITH A THIN PLASMA MIRROR

PLASMA SHEET THICKNESS IS 1/3 THE WAVELENGTH OF THE INCIDENT MICROWAVE RADIATION

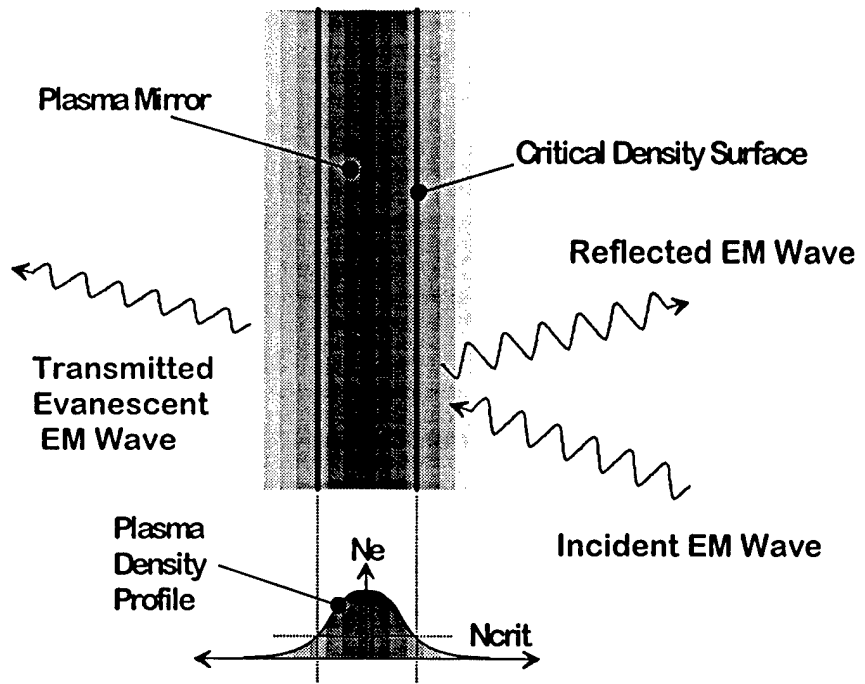


Figure 1. Microwaves are nominally reflected from the critical density surface inside the plasma. If the plasma is thin compared to the wavelength of the incident radiation, then evanescent wave can penetrate the plasma sheet and be detected on the far side at frequencies lower than the plasma frequency.

## TUBULAR CATHODE OPERATING MODES $V_{charge}=2600V$ , 60cm AK gap, OXYGEN FILL

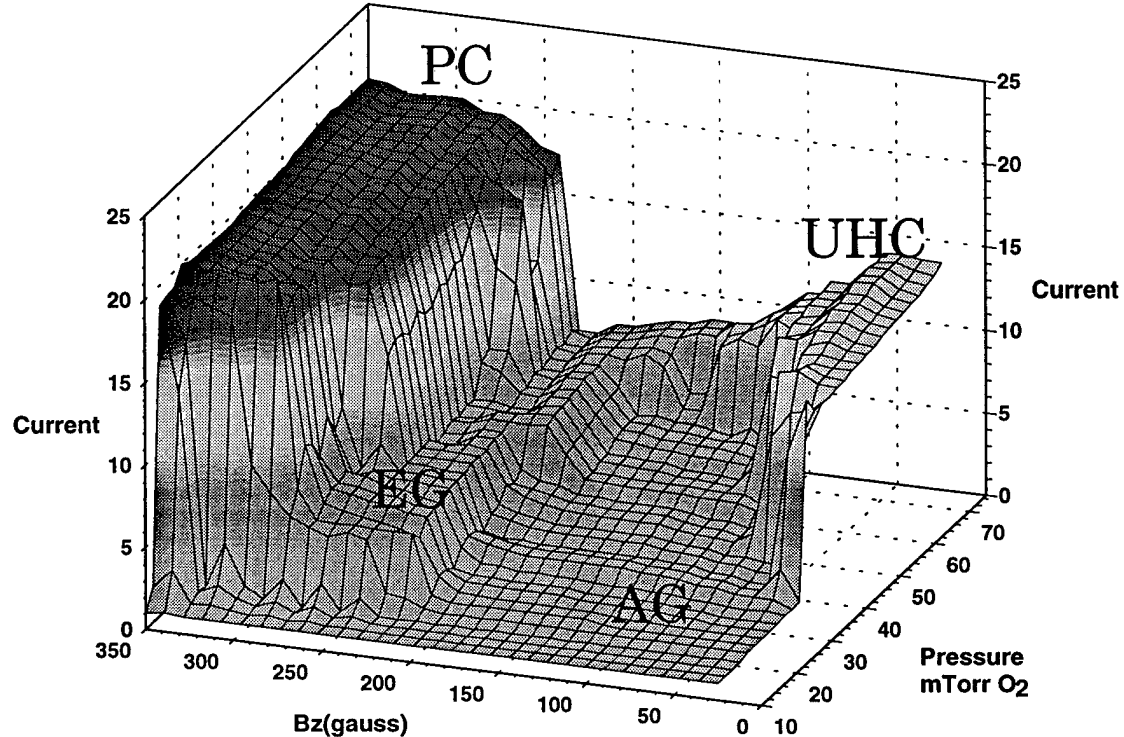


Figure 2. A plot of the current versus the external magnetic field and the gas pressure for the Agile Mirror system.

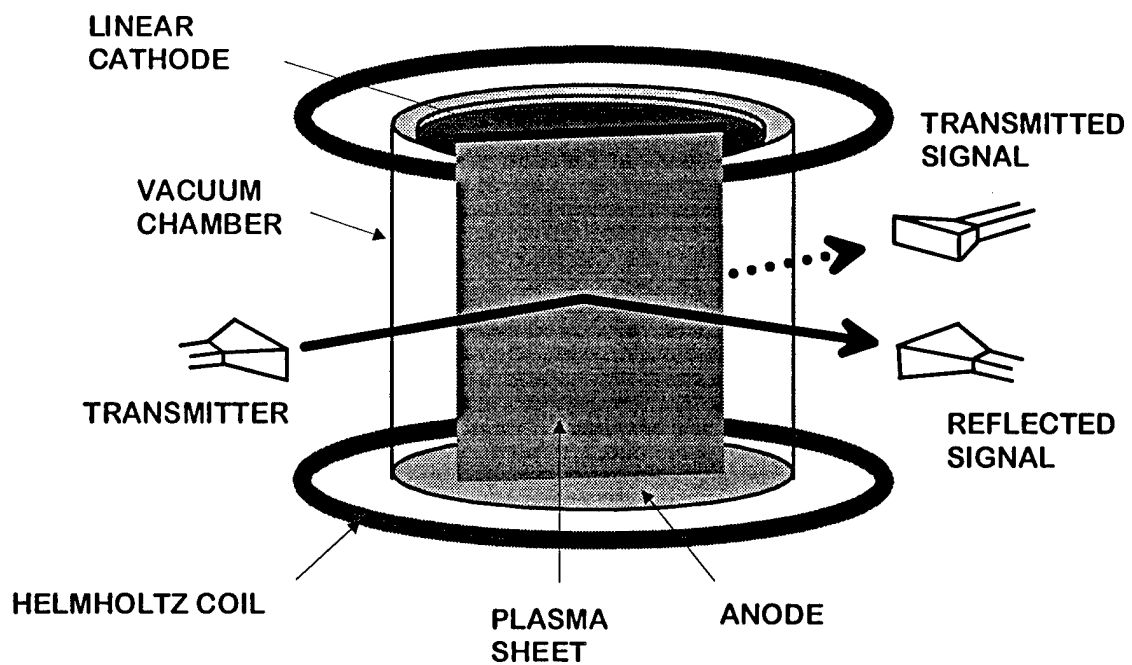


Figure 3. A depiction of the microwave transmission and reflection measurements experimental setup.

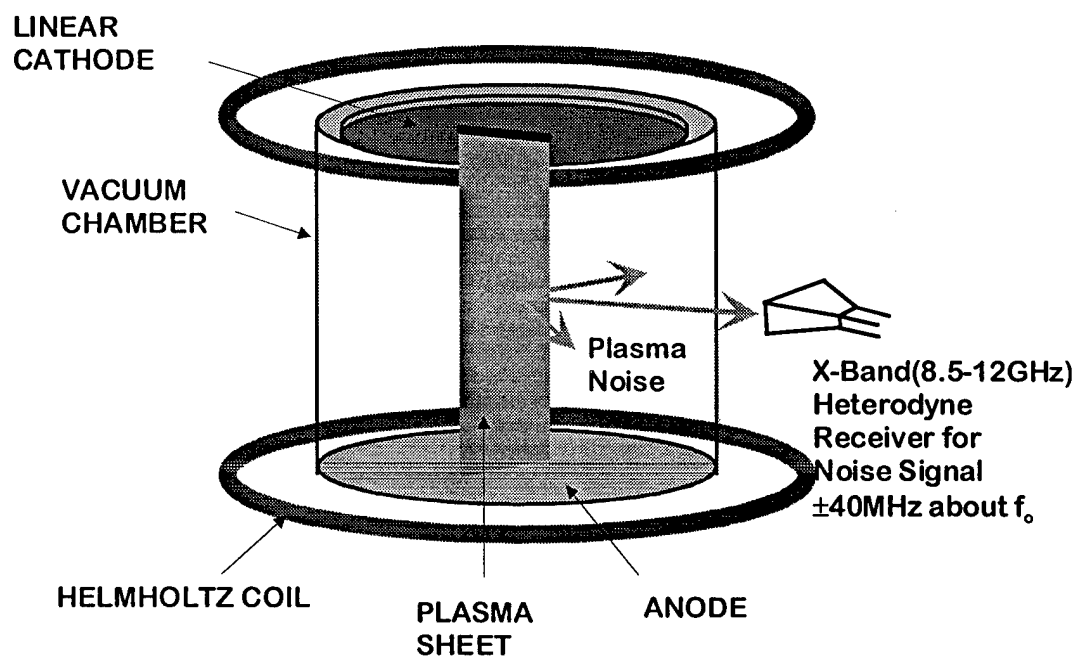
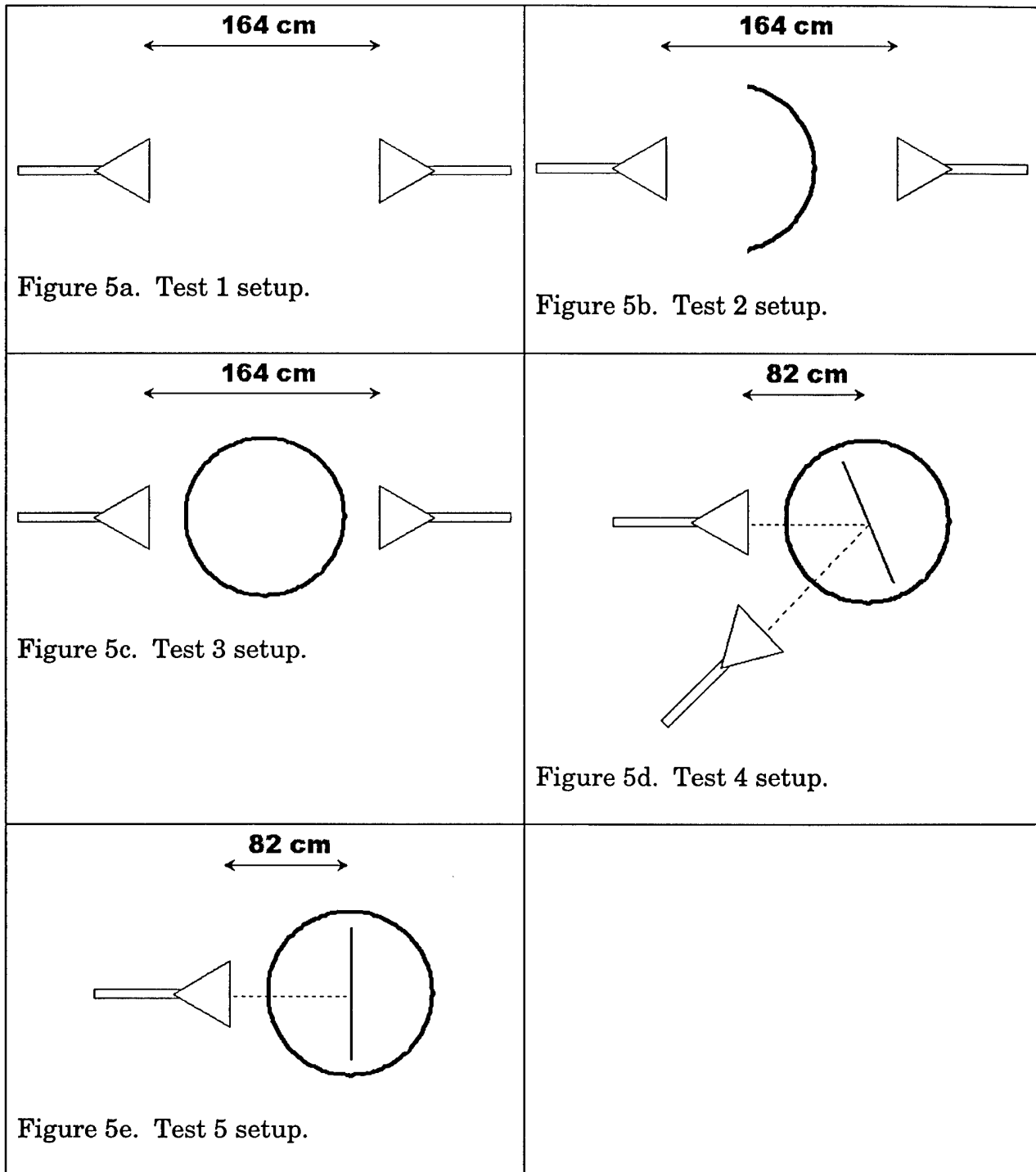


Figure 4. A depiction of the microwave noise measurement experimental setup.



Figures 5a-e. Experimental arrangements for the five part test of reflected microwaves without a sheet plasma present.

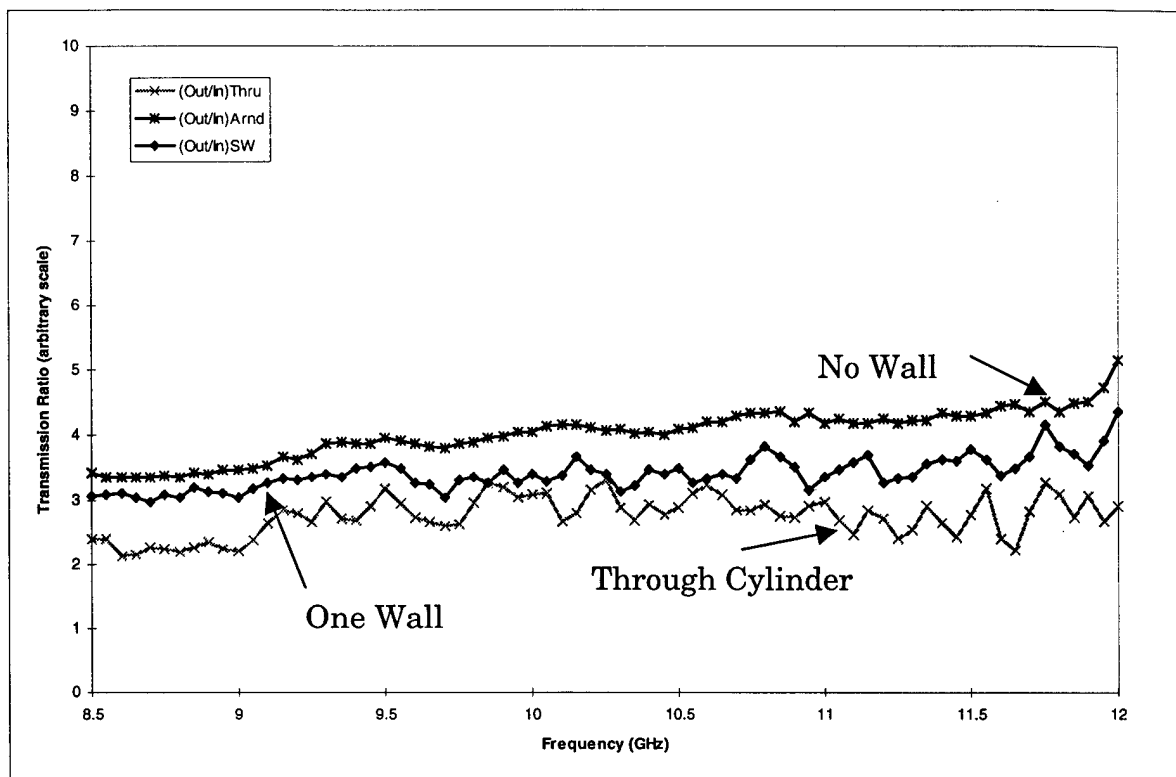


Figure 6a. A plot of microwave transmission in the Agile Mirror system.

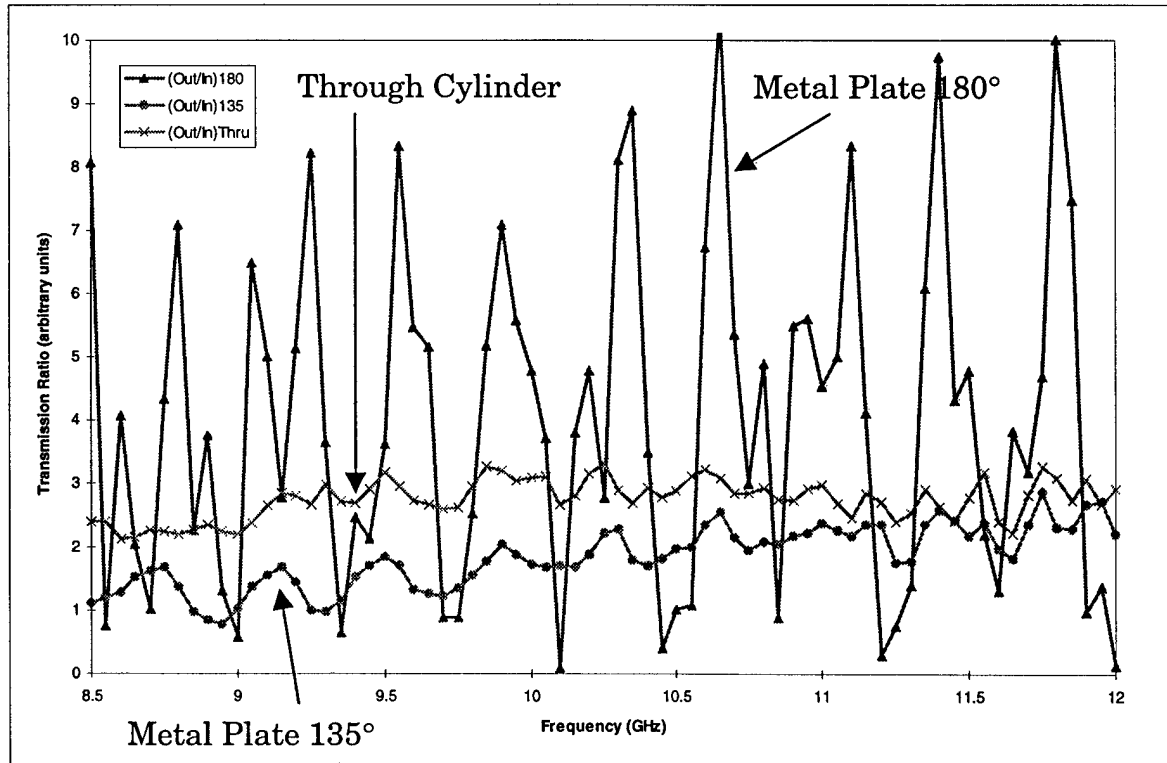


Figure 6b. A plot of microwave signals for various conditions.

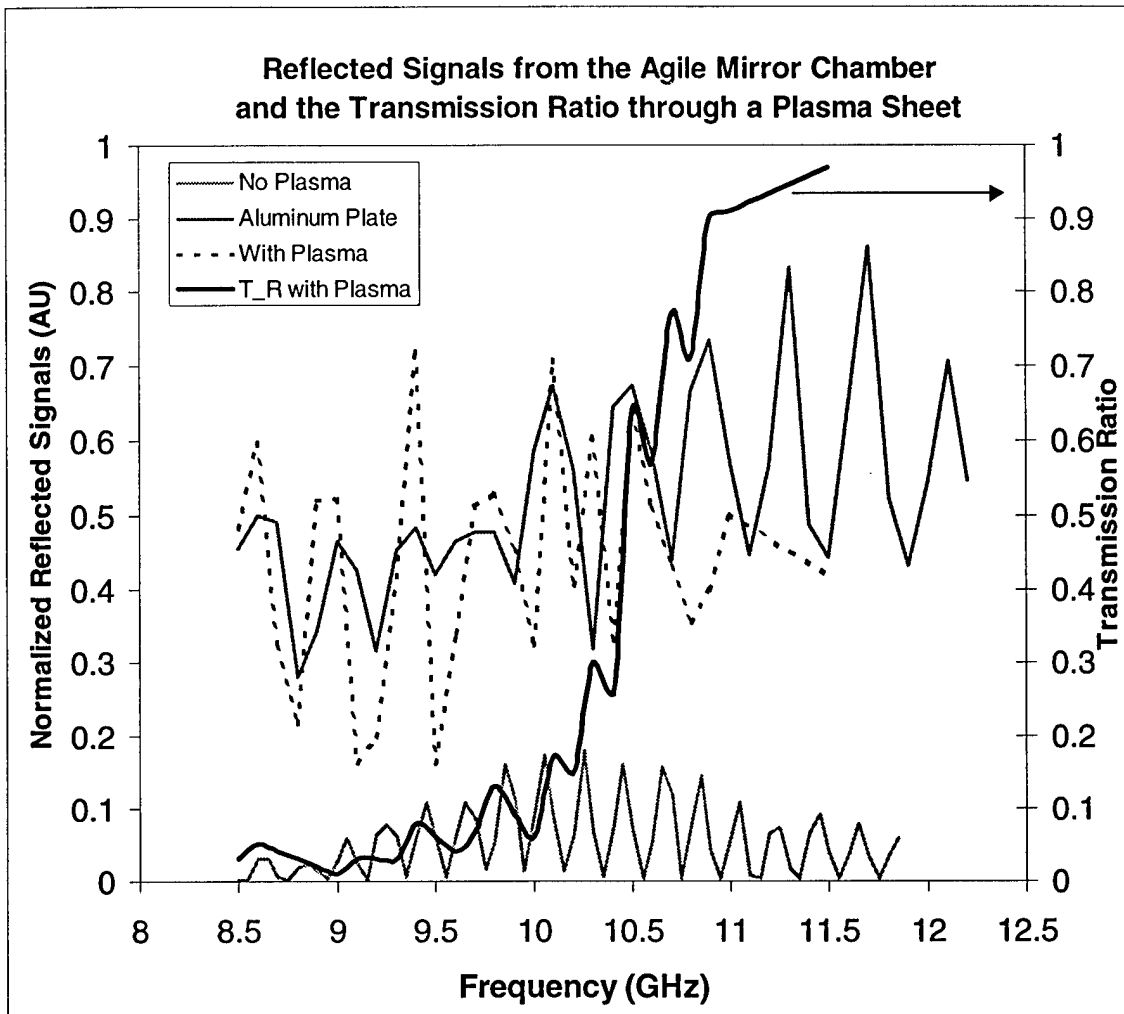


Figure 7. A plot showing the transmission ratio through an EG mode plasma and the reflected signal from the same plasma sheet. Also shown are the measured reflected signals from the chamber without a plasma present and from a solid aluminum plate that is substituted for the plasma. The plasma sheet and the aluminum sheet were rotated  $22.5^\circ$  to the normal vector from the source horn. The included angle between the source horn and the reflected signal horn is  $45^\circ$ . The included angle between the source horn and the transmitted signal horn is  $180^\circ$ .

# PLASMA MICROWAVE NOISE

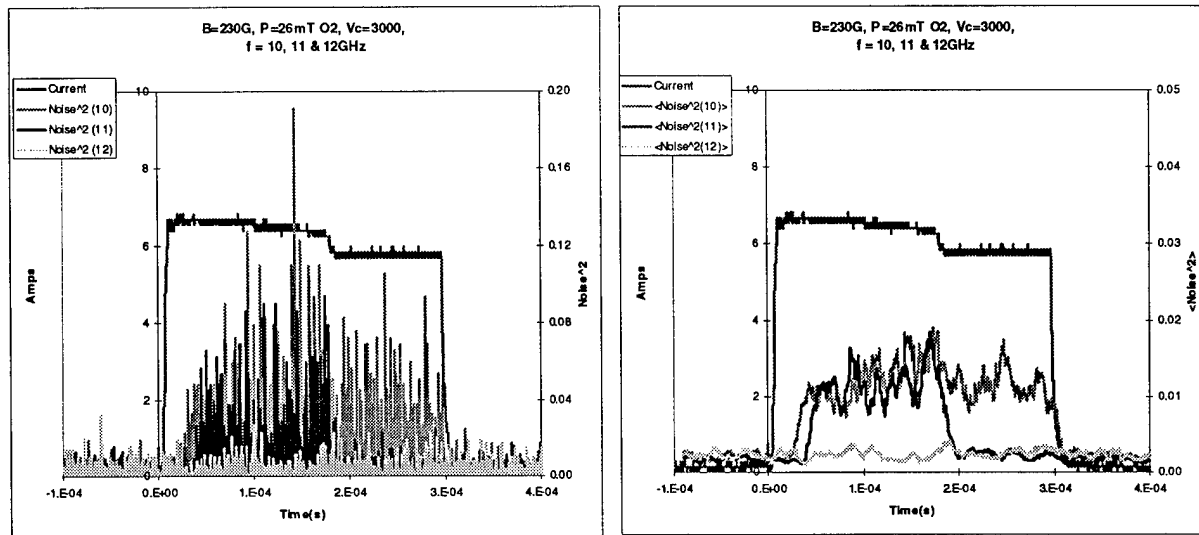


Figure 8. Two graphs of microwave noise for an EG mode plasma. On the left is plotted the square of the noise signal at each time step at various frequencies along with the plasma current. In the right graph the individual noise data points have been replaced with 50-point running averages (10  $\mu$ s averages).

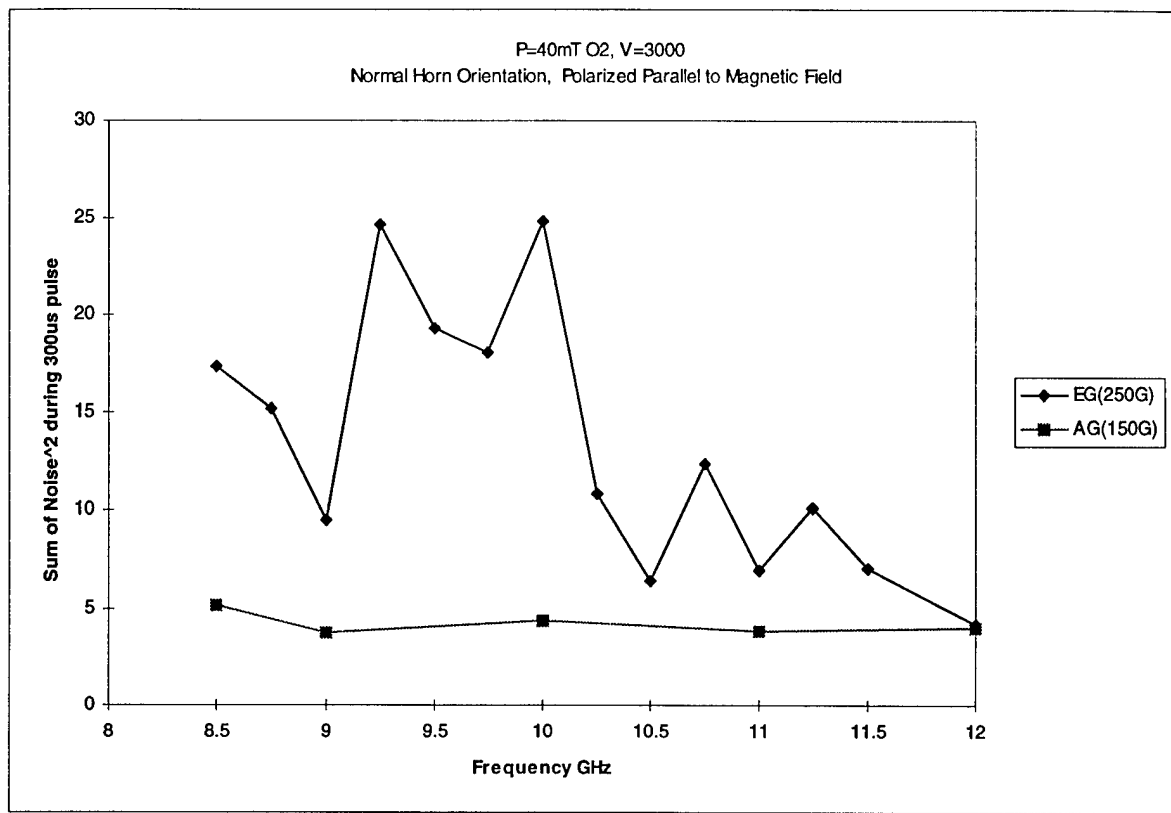


Figure 9. A plot of the total microwave noise emitted during a pulse as a function of frequency for an AG mode plasma and for an EG mode plasma.

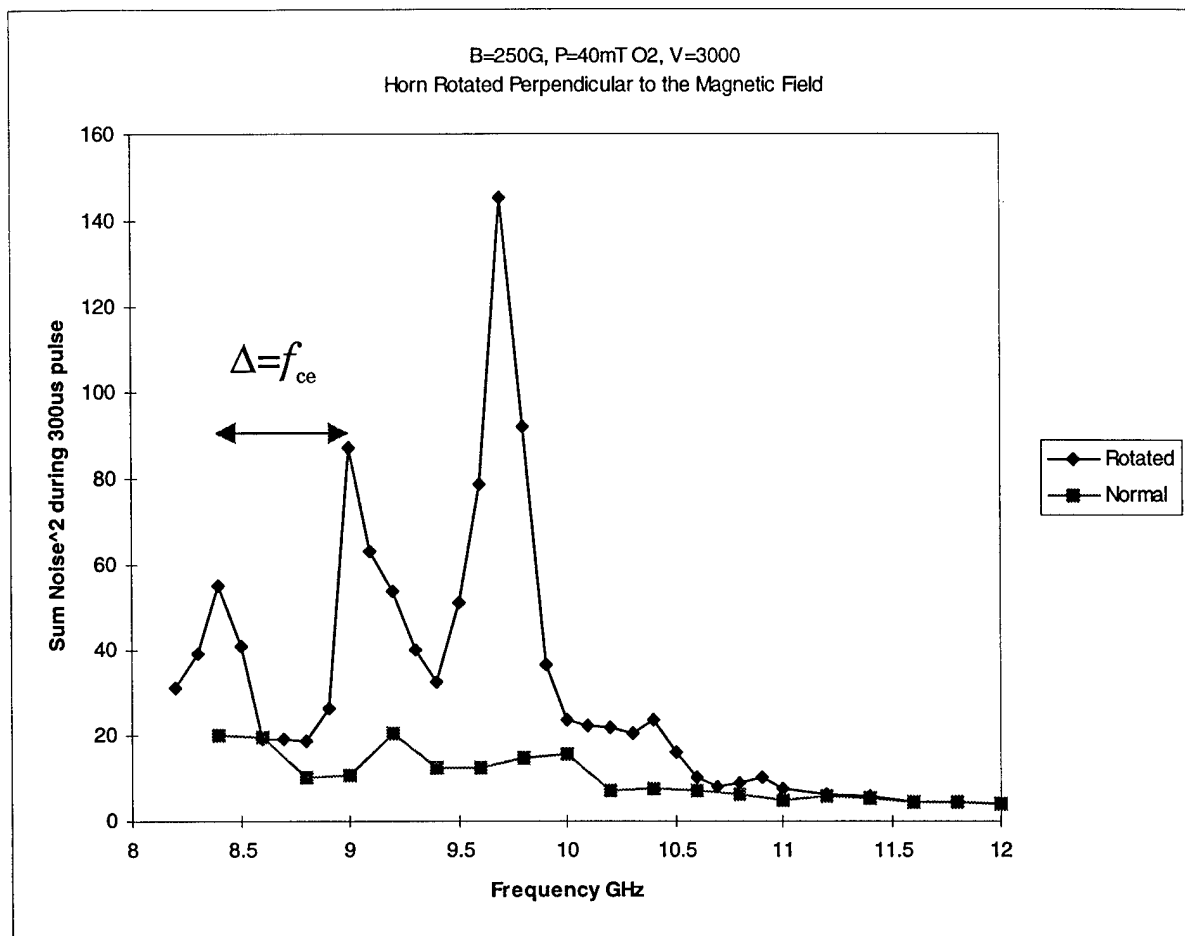


Figure 10. A plot of the total microwave noise emitted during a pulse as a function of frequency for an EG mode plasma. The lower trace is for noise emitted polarized parallel to the external magnetic field and the upper trace is for noise emitted polarized perpendicular to the magnetic field. The spacing between peaks corresponds to harmonics of the electron gyrofrequency.

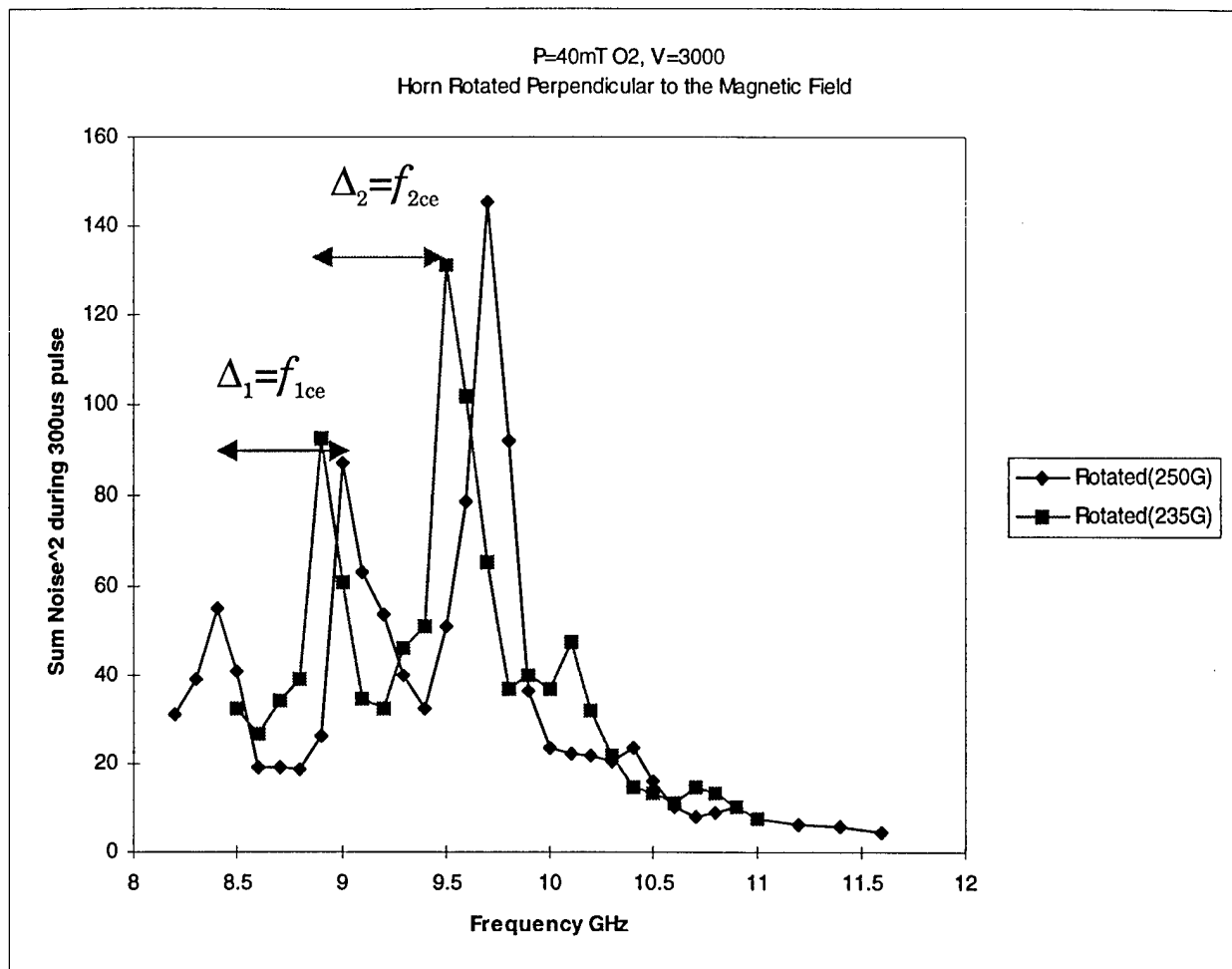


Figure 11. A plot of the total microwave noise emitted polarized perpendicular to the external magnetic field during a pulse as a function of frequency for two EG mode plasmas. The peaks in the 235 gauss data is shifted to lower frequencies and have a smaller peak-to-peak interval relative to the 250 gauss data.

<sup>1</sup> Crossatron is a registered trademark of Hughes Aircraft Company.

<sup>2</sup> J. Mathew, Rev. Sci. Instrum. **65**, 3756 (1994).

<sup>3</sup> R. F. Fernsler, W. M. Manheimer, R. A. Meger, J. Mathew, D. P. Murphy, R. E. Pechacek and J. A. Gregor, Phys. Plamsas **5**, 2137 (1998).

<sup>4</sup> D. R. Corson & P. Lorrain, *Introduction to Electromagnetic Fields and Waves*, W. H. Freeman and Co., San Francisco (1962), p392-396.

<sup>5</sup> J. D. Jackson, *Classical Electrodynamics*, John Wiley & Sons, Inc., New York (1962), p227.